

Evidence from Disrupted Halo Dwarfs that r -process Enrichment via Neutron Star Mergers is Delayed by $\gtrsim 500$ Myrs

ROHAN P. NAIDU,¹ ALEXANDER P. JI,^{2,3} CHARLIE CONROY,¹ ANA BONACA,⁴ YUAN-SEN TING (丁源森),^{5,6} DENNIS ZARITSKY,⁷ LIEKE A. C. VAN SON,¹ FLOOR S. BROEKGAARDEN,¹ SANDRO TACCHHELLA,⁸ VEDANT CHANDRA,¹ NELSON CALDWELL,¹ PHILLIP CARGILE,¹ AND JOSHUA S. SPEAGLE (沈佳士)^{9,10,11,*}

¹Center for Astrophysics | Harvard & Smithsonian, 60 Garden Street, Cambridge, MA 02138, USA

²Department of Astronomy & Astrophysics, University of Chicago, 5640 S Ellis Avenue, Chicago, IL 60637, USA

³Kavli Institute for Cosmological Physics, University of Chicago, Chicago, IL 60637, USA

⁴Observatories of the Carnegie Institution for Science, 813 Santa Barbara St., Pasadena, CA 91101, USA

⁵Research School of Astronomy & Astrophysics, Mount Stromlo Observatory, Cotter Road, Weston Creek, ACT 2611, Canberra, Australia

⁶Research School of Computer Science, Australian National University, Acton ACT 2601, Australia

⁷Steward Observatory, University of Arizona, 933 North Cherry Avenue, Tucson, AZ 85721-0065, USA

⁸Department of Physics, Ulsan National Institute of Science and Technology (UNIST), Ulsan 44919, Republic of Korea

⁹David A. Dunlap Department of Astronomy & Astrophysics, University of Toronto, 50 St. George Street, Toronto ON M5S 3H4, Canada

¹⁰Dunlap Institute for Astronomy and Astrophysics, University of Toronto, 50 St George Street, Toronto, ON M5S 3H4, Canada

¹¹Department of Statistical Sciences, University of Toronto, 100 St George St, Toronto, ON M5S 3G3, Canada

ABSTRACT

The astrophysical origins of r -process elements remain elusive. Neutron star mergers (NSMs) and special classes of core-collapse supernovae (rCCSNe) are leading candidates. Due to these channels' distinct characteristic timescales (rCCSNe: prompt, NSMs: delayed), measuring r -process enrichment in galaxies of similar mass, but differing star-formation durations might prove informative. Two recently discovered disrupted dwarfs in the Milky Way's stellar halo, Kraken and *Gaia*-Sausage Encladus (GSE), afford precisely this opportunity: both have $M_\star \approx 10^8 M_\odot$, but differing star-formation durations of ≈ 2 Gyrs and ≈ 3.6 Gyrs. Here we present $R \approx 50,000$ Magellan/MIKE spectroscopy for 31 stars from these systems, detecting the r -process element Eu in all stars. Stars from both systems have similar $[\text{Mg}/\text{H}] \approx -1$, but Kraken has a median $[\text{Eu}/\text{Mg}] \approx -0.1$ while GSE has an elevated $[\text{Eu}/\text{Mg}] \approx 0.2$. With simple models we argue NSM enrichment must be delayed by 500 – 1000 Myrs to produce this difference. rCCSNe must also contribute, especially at early epochs, otherwise stars formed during the delay period would be Eu-free. In this picture, rCCSNe account for $\approx 50\%$ of the Eu in Kraken, $\approx 25\%$ in GSE, and $\approx 15\%$ in dwarfs with extended star-formation durations like Sagittarius. The inferred delay time for NSM enrichment is 10 – 100 \times longer than merger delay times from stellar population synthesis – this is not necessarily surprising because the enrichment delay includes time taken for NSM ejecta to be incorporated into subsequent generations of stars. For example, this may be due to natal kicks that result in r -enriched material deposited far from star-forming gas, which then takes $\approx 10^8 - 10^9$ years to cool in these galaxies.

Keywords: Galaxy: halo — Galaxy: kinematics and dynamics — Galaxy: evolution — Galaxy: formation — Galaxy: stellar content

1. INTRODUCTION

Approximately half the elements in the modern periodic table originate in the rapid neutron capture process (r -process, see Cowan et al. 2021 for a recent review). Despite this outsized importance, the astrophys-

ical birth-sites of the r -process remain elusive. Neutron star mergers (NSMs) and special classes of core-collapse supernovae (rCCSNe¹) are leading candidates. The one NSM witnessed via electromagnetic radiation (GW170817) has shown signatures of r -process produc-

Corresponding author: Rohan P. Naidu
rohan.naidu@cfa.harvard.edu

* Banting & Dunlap Fellow

¹ We use “rCCSNe” to denote the special core-collapse supernovae that produce r -process elements (e.g., hypernovae, magnetorotational supernovae, magnetars), and “CCSNe” to reference the entire population of core-collapse supernovae.

tion (e.g., Kasen et al. 2017; Drout et al. 2017; Kasliwal et al. 2017), but NSMs alone might be unable to explain features of r -process chemistry observed in the Milky Way (MW) and its dwarf galaxies (e.g., Côté et al. 2019; Haynes & Kobayashi 2019; Reichert et al. 2020; Skúladóttir & Salvadori 2020; Tsujimoto 2021). On the other hand, rCCSNe such as magnetorotational hypernovae have been theorized as feasible channels, but empirical evidence remains tentative (e.g., Ting et al. 2012; Nishimura et al. 2017; Halevi & Mösta 2018; Siegel et al. 2019; Kobayashi et al. 2020; Yong et al. 2021).

Here we seek new constraints on the r -process from the stellar halo. The key development in the last few years, enabled by the *Gaia* mission, has been the identification of the distinct dwarf galaxies whose debris constitutes the halo (e.g., Belokurov et al. 2018; Helmi et al. 2018; Myeong et al. 2019; Koppelman et al. 2019; Yuan et al. 2020; Kruijssen et al. 2020; Naidu et al. 2020; Horta et al. 2021). Like some of the MW’s surviving dwarfs, some disrupted dwarfs are also chemical fossils – they formed all their stars in the first few Gyrs of the Universe before they were tidally disrupted by the Galaxy. The most ancient surviving dwarfs have been studied for decades to isolate the imprints of the r -process since they are enriched only by a few generations of star-formation (e.g., Ji et al. 2016a; Duggan et al. 2018; Skúladóttir et al. 2019). Now we turn to the ancient disrupted dwarfs, whose unique characteristics are particularly suited to unraveling the r -process.

Of particular importance, debris from multiple $M_\star \gtrsim 10^8 M_\odot$ systems has been identified within a few kpc from the Sun (e.g., from the *Gaia*-Sausage Enceladus galaxy accreted at redshift $z \approx 2$, Helmi et al. 2018; Belokurov et al. 2020; Naidu et al. 2021). In this mass regime, stochastic effects due to the expected rarity of production sites (e.g., roughly one NSM expected for $\approx 10^5 M_\odot$, e.g., Ji et al. 2016a) and undersampling of the initial mass function (e.g., Koch et al. 2008) do not complicate the interpretation of r -process chemistry unlike in low mass dwarf galaxies. Accounting for shallow potential wells that are unable to hold on to enriched gas is also no longer an issue (e.g., GSE had a total mass $\approx 2 \times 10^{11} M_\odot$, Naidu et al. 2021).

A practical advantage is that some disrupted dwarfs are the “nearest” dwarf galaxies, since their debris circulates through the Solar neighborhood and is easily within the grasp of high-resolution spectroscopy. Low and high-resolution spectra for tens of thousands of GSE stars have already been acquired, making it the most spectroscopically studied dwarf galaxy of all time (e.g., Steinmetz et al. 2020; Bird et al. 2019; Conroy et al. 2019; Mackereth & Bovy 2020; Buder et al. 2021) though only a small fraction of these spectra are currently able to support r -process studies due to the signal-to-noise, resolution, and wavelength coverage required (e.g., Aguado et al. 2020; Matsuno et al. 2021).

Another useful feature of the disrupted dwarfs is that many independent chemo-dynamical methods may be deployed to determine their star-formation (SF) duration, which is crucial in disentangling “delayed” sources of enrichment like NSMs from “prompt” sources like rCCSNe. By SF duration we mean the period over which a galaxy has assembled the bulk of its stellar mass. SF durations are being inferred from diverse methods such as: age distributions from spectra of hundreds of *individual* main-sequence turnoff stars (e.g., Bonaca et al. 2020), color magnitude diagram fitting (e.g., Gallart et al. 2019), tailored merger simulations (e.g., Naidu et al. 2021), orbital signatures (e.g., Pfeffer et al. 2020), and ages/metallicities of accompanying GC systems (e.g., Kruijssen et al. 2019).

In this paper we constrain the channels of r -process enrichment by contrasting GSE and Kraken, two of the most massive dwarfs to have merged with the Milky Way. These galaxies have similar stellar and halo masses, but different star-formation durations, thereby affording a controlled experiment to disentangle the r -process contributions of rCCSNe and NSMs. We select GSE and Kraken samples from APOGEE DR16 (§2), describe our Magellan/MIKE followup (§3), discuss the mass and star-formation durations of GSE and Kraken (§4), present the MIKE abundances (§5), interpret them with simple chemical evolution models (§6), and close by discussing the implications of our results (§7). We use r_{gal} to denote the total Galactocentric distance, E_{tot} for the total orbital energy, and e for the eccentricity of orbits. We adopt a Planck Collaboration et al. (2018) cosmology to convert redshifts into lookback times.

2. SAMPLE SELECTION

The samples studied here were selected from APOGEE DR16 (Jönsson et al. 2020) cross-matched with *Gaia* EDR3 (Gaia Collaboration et al. 2021). We adopt data quality cuts for APOGEE following Horta et al. (2021) and *Gaia* EDR3 following Gaia Collaboration et al. (2021). Globular cluster (GC) member stars are excluded based on radial velocity and proper motion cuts – 3σ around the mean cluster radial velocity and proper motions for stars lying within $3\times$ the tidal radius of the cluster on-sky. GC parameters are sourced from Baumgardt & Hilker (2018); Baumgardt et al. (2019); Vasiliev & Baumgardt (2021). Distances to stars beyond ≈ 3 kpc from the Sun, especially towards the Galactic center, are uncertain based on *Gaia* parallaxes alone so we rely on data-driven distances fit to these stars from Leung & Bovy (2019) and an updated version of Hogg et al. (2019); Eilers et al. (2019) based on DR16 and *Gaia* EDR3 (A.C. Eilers, private comm.), discarding stars for which these authors’ distances disagree by $> 1\sigma$. With full 6D phase-space coordinates from these datasets, we are able to compute dynamical quantities of interest (angular momenta, energies, eccentricities) following Naidu et al. (2020). We use these quantities

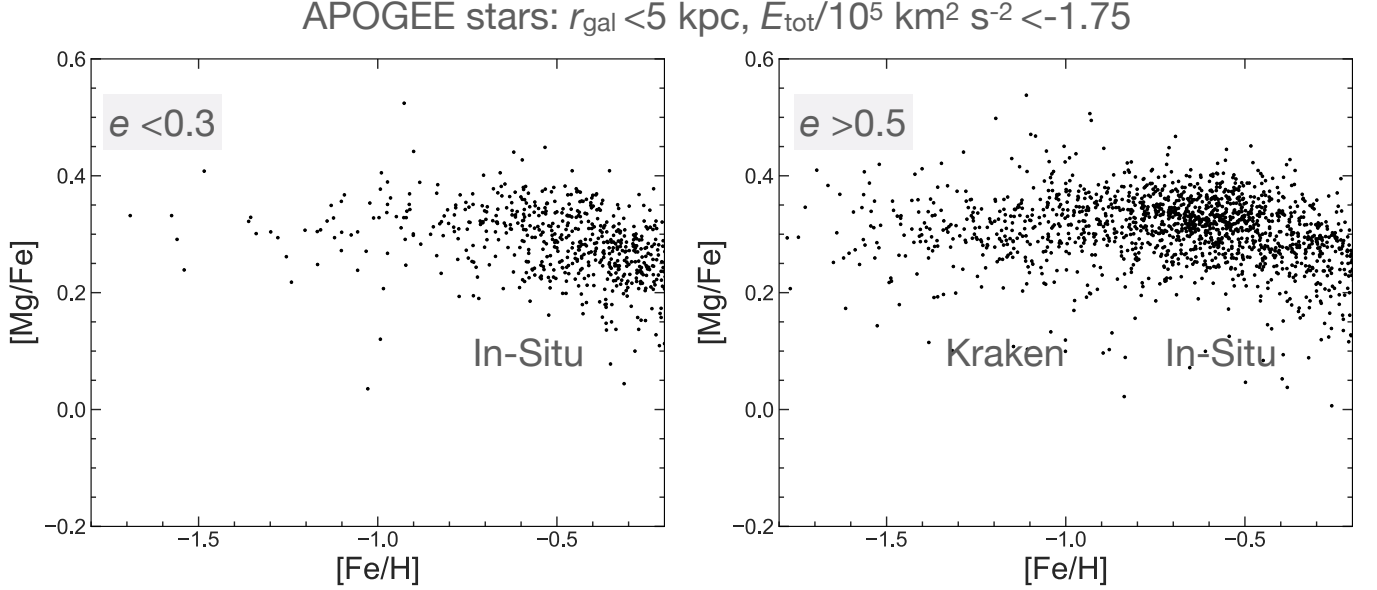


Figure 1. Revealing Kraken in the APOGEE dataset. $[\text{Mg}/\text{Fe}]$ vs. $[\text{Fe}/\text{H}]$ for APOGEE stars in the inner 5 kpc of the Galaxy selected to have low energy (energy cut from Fig. 2). The eccentric stars (right panel) show a metal-poor, Mg-enhanced population that is absent at lower eccentricities (left panel). This preferential concentration at $e > 0.5$ tracks the Kraken GCs and is expected from dynamical friction considerations for a high mass-ratio merger (e.g., Naidu et al. 2021).

along with APOGEE abundances to design our Kraken and GSE selections.

2.1. Kraken

From the clustering of a dozen GCs in the age-metallicity plane as well as various dynamical planes, it has been inferred that the remains of a massive ($M_{\star} \gtrsim 10^8 M_{\odot}$) dwarf galaxy (“Kraken”) lies buried in the inner few kpc of the MW (e.g., Kruijssen et al. 2019; Massari et al. 2019; Forbes 2020; Pfeffer et al. 2021). The sheer number of GCs, and the fact that they are confined to the inner regions of the Galaxy (apocenters $\lesssim 5 \text{ kpc}$) has been interpreted as evidence for an early accretion event ($z \gtrsim 2$) that was likely the MW’s highest mass-ratio merger (Kruijssen et al. 2020).

Almost all GCs associated with Kraken in the age-metallicity plane (e.g., Kruijssen et al. 2019) lie at $r_{\text{gal}} \lesssim 5 \text{ kpc}$ and are eccentric ($\langle e \rangle \approx 0.75$), as expected for a massive merger wherein the infalling galaxy is rapidly radialized due to efficient dynamical friction (e.g., Amorisco 2017; Koppelman et al. 2020; Naidu et al. 2021; Vasiliev et al. 2021). Supporting the existence of Kraken, even low-energy field stars at $< 5 \text{ kpc}$ show a metal-poor sequence that preferentially occurs on radial orbits ($e > 0.5$, Figure 1). Importantly, this population does not define a continuous distribution in eccentricity, and preferentially occurs at $e > 0.5$. This distribution mirrors the Kraken GCs. Further, it is evidence that we are not observing an in-situ population like the splashed disk that has a continuous eccentricity

distribution (e.g., Bonaca et al. 2020; Belokurov et al. 2020).

Empirically, the $[\text{Mg}/\text{Mn}]$ vs. $[\text{Al}/\text{Fe}]$ plane has been shown to separate accreted stars from in-situ MW stars (Hawkins et al. 2015; Das et al. 2020; Horta et al. 2021). In Figure 2 we select accreted stars based on this plane and find these stars separate into two clear subsets – one at high energy, consistent with GSE (e.g., Naidu et al. 2020) and another at low energy, exactly where the Kraken GCs are found to cluster (e.g., Massari et al. 2019). Further, the low-energy accreted stars define a coherent sequence in the $[\text{Fe}/\text{H}]$ vs. $[\text{Mg}/\text{Fe}]$ plane characteristic of a single dwarf galaxy that is distinct from GSE. The elevated $[\text{Mg}/\text{Fe}] \approx 0.3$ of this sequence is consistent with a galaxy disrupted before Type Ia supernovae began dominating chemical evolution.

In summary, the chemodynamical signatures of the Kraken dwarf galaxy inferred from GCs are closely mirrored by a population of stars in the inner Galaxy that we select as follows:

$$\begin{aligned}
 & (r_{\text{gal}}/[\text{kpc}] < 5) \wedge (e > 0.5) \\
 & \quad \wedge [\text{Mg}/\text{Mn}] > 0.25 \\
 & \wedge [\text{Mg}/\text{Mn}] - 4.25[\text{Al}/\text{Fe}] > 0.55 \\
 & \quad \wedge E_{\text{tot}}/[10^5 \text{ km}^2 \text{ s}^{-2}] < -1.75.
 \end{aligned} \tag{1}$$

We end this subsection by noting that Kraken has been identified under other names in the literature – the host of the “low-energy” GCs (Massari et al. 2019), “Koala” (Forbes 2020), and “Inner Galaxy Structure”/“Heracles” (Horta et al. 2021). Given the close

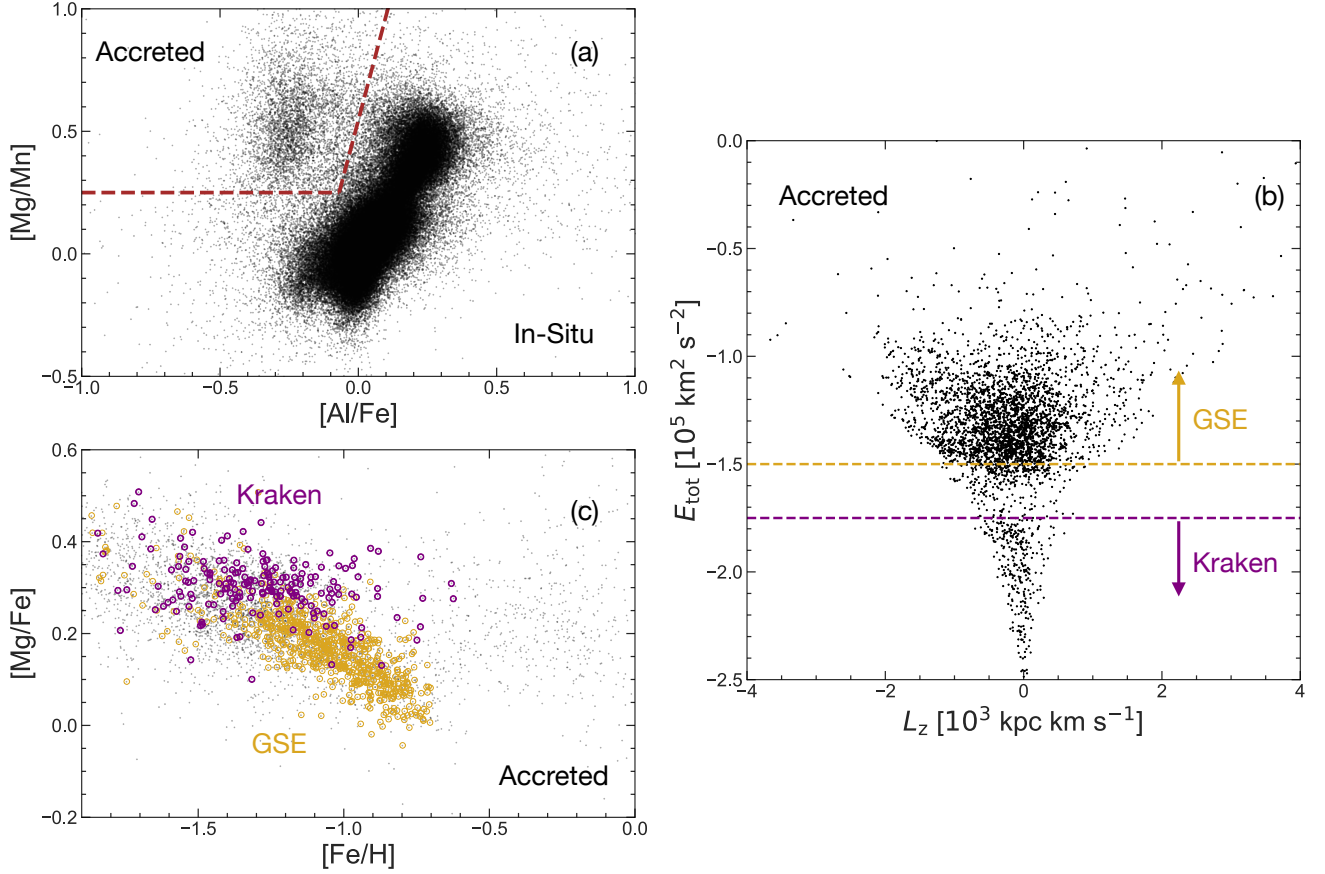


Figure 2. Selecting Kraken and GSE samples. **Panel (a):** All APOGEE stars that satisfy our quality cuts are shown in the [Mg/Mn] vs. [Al/Fe] chemical plane that has been used to separate accreted stars from in-situ stars (e.g., Das et al. 2020). We use the brown dashed line to demarcate the two visibly distinct populations. **Panel (b):** Total orbital energy vs. the z -component of angular momentum for accreted stars identified via Panel (a). There is a clear gap around $E_{\text{tot}} \approx -1.6 \times 10^5 \text{ km}^2 \text{ s}^{-2}$ between a high energy population (GSE) and a low energy population (Kraken). **Panel (c):** The final selected Kraken (purple) and GSE (golden) samples (see Eqns. 1, 2) show tight, coherent [Mg/Fe] vs. [Fe/H] sequences characteristic of distinct dwarfs. The Kraken sequence is α -enhanced with no visible “knee”, which is expected for a galaxy disrupted earlier, and forming stars more efficiently than GSE.

correspondence in the properties of our selected stars and the Kruijssen et al. (2020) Kraken GCs, we are confident our criteria select the stellar debris of the Kraken dwarf galaxy.

2.2. Gaia-Sausage Enceladus (GSE)

To select a pure GSE sample we focus on eccentric, accreted stars as identified in the [Mg/Mn] vs. [Al/Fe] plane at energies and distances larger than Kraken motivated by Figure 2:

$$\begin{aligned}
 & (r_{\text{gal}}/[\text{kpc}] > 5) \wedge (e > 0.7) \\
 & \quad \wedge [\text{Mg/Mn}] > 0.25 \\
 & \wedge [\text{Mg/Mn}] - 4.25[\text{Al/Fe}] > 0.55 \\
 & \quad \wedge E_{\text{tot}}/[10^5 \text{ km}^2 \text{ s}^{-2}] > -1.50.
 \end{aligned} \tag{2}$$

These criteria are very similar in spirit to typical literature selections of GSE (see Buder et al. 2021 for a compilation). The median abundances ([Fe/H] and [Mg/Fe]) are in excellent agreement with Naidu et al. (2020), who did not make cuts in the [Mg/Mn] vs. [Al/Fe] plane. Further note that the Naidu et al. (2020) sample measures metallicities down to $[\text{Fe/H}] \approx -3.0$, and so the agreement in medians is an important check that the metallicity distribution function (MDF) sampled by APOGEE is not meaningfully distorted by the lack of coverage at $[\text{Fe/H}] \lesssim -2.0$.

3. OBSERVATIONS AND ABUNDANCE ANALYSIS

We observed 20 Kraken stars and 11 GSE stars with Magellan/MIKE (Bernstein et al. 2003) on 27-29 July 2021 with the $0''.5$ slit and 2×1 binning, providing resolu-

tion $R \approx 50,000/40,000$ on the blue/red arm of MIKE, respectively that span 3300-5000 Å and 4900-10,000 Å. These stars were selected based on their brightness and observability from Magellan from those satisfying Eqns. 1 and 2. The data were reduced with CarPy (Kelson 2003). The spectra were analyzed using SMHR², which provides an interface to doppler correct, normalize and stitch orders, fit equivalent widths, interpolate Castelli & Kurucz (2004) stellar atmospheres, and run MOOG including scattering opacity (Snedden 1973; Sobeck et al. 2011) and Barklem et al. (2000) damping³ to determine abundances from equivalent widths and spectrum synthesis (see Ji et al. 2020 for a detailed description).

The analyzed lines were selected primarily from Jönsson et al. (2017), Lomaeva et al. (2019), and Forsberg et al. (2019), who selected good unblended lines for metal-rich red giant stars in the disk and bulge. We supplemented these lists with lines selected by Roederer et al. (2018), both to measure more elements and to replace lines that were undetected in any of our stars. For Fe I, Fe II, O I, Mg I, Ca I, and Ti I, we adopted the atomic data from Jönsson et al. (2017) when available to ensure our stellar parameters and α -abundances are on the same scale as their results. The atomic data for other species (Na I, Al I, Si I, K I, Sc II, V I, Mn I, Ni I, Zn I, Y II, Ba II, La II, Ce II, Eu II) were taken from linemake (Placco et al. 2021), which keeps up-to-date libraries of experimentally measured oscillator strengths.

Stellar parameters were determined by balancing excitation potential vs. Fe I abundance for T_{eff} , ionization balance for Fe I and II for $\log g$, line strength vs. Fe I abundance for ν_t , and setting the model metallicity to [Fe/H]. We adopted $[\alpha/\text{Fe}] = +0.4$ atmospheres for the analysis, but we verified that the results and conclusions are unchanged for $[\alpha/\text{Fe}] = 0.0$. Since we used the same Fe lines as Jönsson et al. (2017), we adopted their systematic uncertainties of 50 K, 0.15 dex, 0.10 km s^{-1} , and 0.05 dex for T_{eff} , $\log g$, ν_t , and [M/H] respectively. Statistical uncertainties were determined using the standard error on the respective slopes or abundance differences. Stellar parameter uncertainties were propagated to abundance uncertainties following Ji et al. (2020).

4. MASS & STAR-FORMATION DURATION

Here we discuss two fundamental parameters of Kraken and GSE – mass and star-formation duration – that are crucial to interpreting their chemical evolution.

Both the stellar mass and halo mass of GSE and Kraken have been found to be similar via a variety of methods. For instance, comparing the chemodynamical properties of the accompanying GC systems against

a suite of hydrodynamical MW simulations, Kruijssen et al. (2020) inferred $M_\star = 2.7^{+1.1}_{-0.8} \times 10^8 M_\odot$, $M_{\text{halo}} = 9.6^{+1.6}_{-1.7} \times 10^{10} M_\odot$ for GSE, and $M_\star = 1.9^{+1.0}_{-0.6} \times 10^8 M_\odot$, $M_{\text{halo}} = 8.3^{+2.2}_{-1.7} \times 10^{10} M_\odot$ for Kraken. Other methods yield consistent results and include GC to halo mass relations (GSE & Kraken: Forbes 2020), chemical evolution models (GSE: Fernández-Alvar et al. 2018, Kraken: Horta et al. 2021), tailored N-body simulations (GSE: Naidu et al. 2021), halo star counts (GSE: Mackereth & Bovy 2020), and the mass metallicity relation (assuming high- z evolution of the relation from Ma et al. 2016, and accretion redshifts from Bonaca et al. 2020 and Kruijssen et al. 2020).

Since GSE comprises the bulk of halo stars in the Solar neighborhood, ages for hundreds of GSE main-sequence turnoff stars have been measured via high-resolution spectroscopy combined with optical through IR photometry (Bonaca et al. 2020). The age distributions show virtually all GSE stars to be > 10.2 Gyrs old, with an SF duration of $3.6^{+0.1}_{-0.2}$ Gyrs.

For Kraken, which is buried in the dusty Galactic center and has therefore been studied more sparsely, we rely on less direct tracers. A lower-limit comes from the age-spread of the GCs associated with Kraken (Massari et al. 2019; Kruijssen et al. 2020) – the GC age-spread is 1 Gyr as per Dotter et al. (2010, 2011) and 1.5 Gyr as per VandenBerg et al. (2013). An upper limit comes from observing that Kraken must have been disrupted before GSE owing to its depth in the potential and truncated chemical sequence with no “knee” in the [Fe/H] vs. [Mg/Fe] plane (Figure 2), i.e., Kraken’s SF duration must be < 3.6 Gyr. As our fiducial value we adopt 2 Gyr based on Kruijssen et al. (2020) who used all available information on the Kraken GCs (age, metallicity, dynamics) to infer ≈ 1.7 Gyrs as the difference between GSE and Kraken’s accretion epochs.

The key takeaway from this section is that the similar stellar and halo masses of Kraken and GSE make for a controlled experiment, wherein observed differences in chemistry must arise mainly due to the differing star-formation durations. Almost all physical processes important to chemical evolution are to first order a function of halo mass and the depth of the potential, and must thus be similar in both galaxies (e.g., the fraction of enriched gas lost to outflows, neutron stars that become unbound due to natal kicks). This contrasts with previous studies of r -process enrichment in intact dwarf galaxies (e.g., Duggan et al. 2018; Skúladóttir & Salvadori 2020), which by necessity compare galaxies of very different stellar and halo masses and are more susceptible to galaxy formation uncertainties.

5. ABUNDANCE RESULTS

In Figure 3 we contrast abundances of Eu, Mg, Fe, and Ba measured for Kraken and GSE. The Kraken sample spans [Fe/H] of -2.0 to -1.2 (median: $-1.52^{+0.08}_{-0.03}$) whereas the GSE sample spans [Fe/H] of -1.5 to -1.0

² <https://github.com/andycasey/smhr>, first described in Casey 2014

³ <https://github.com/alexji/moog17scat>

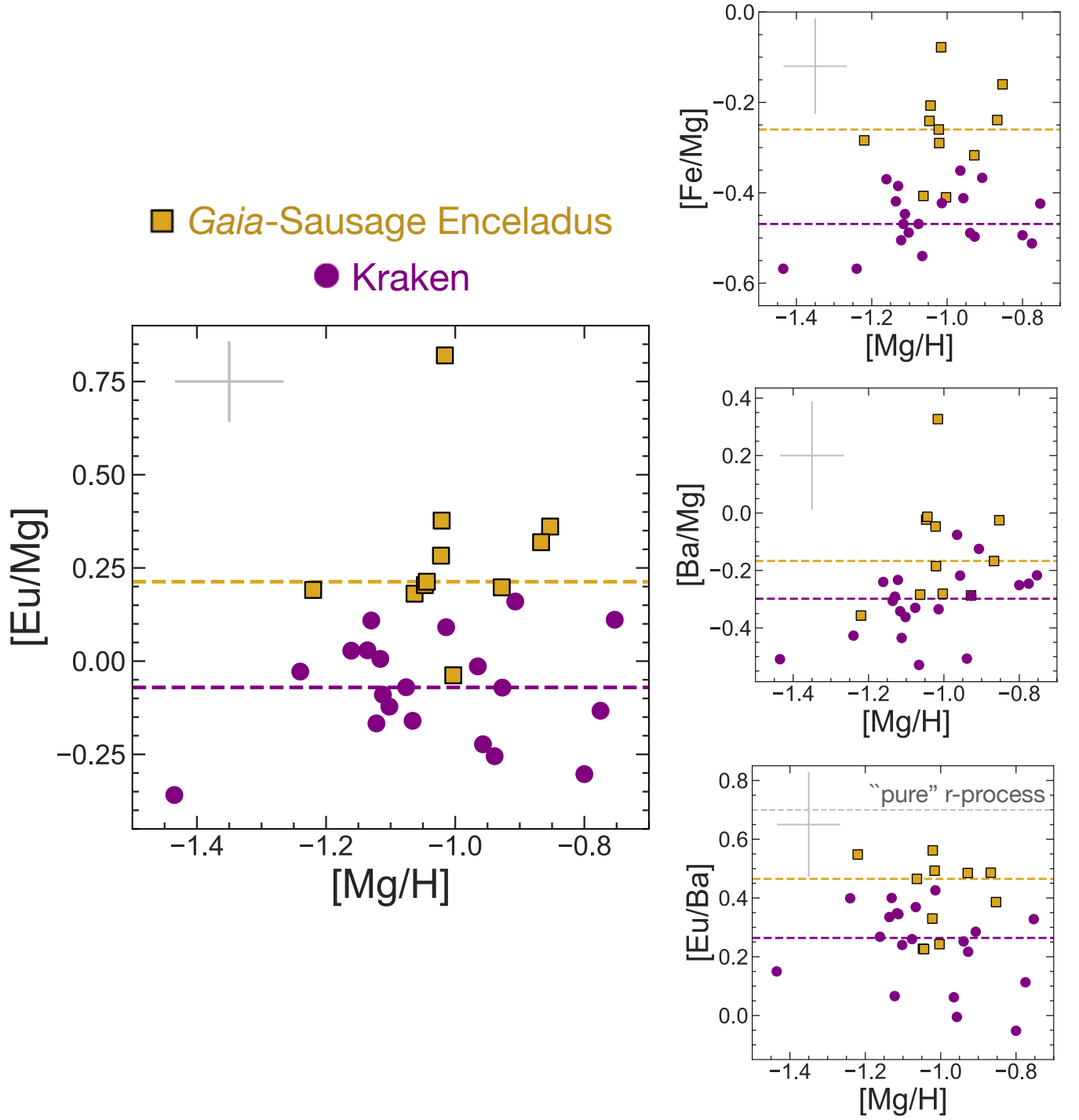


Figure 3. Magellan/MIKE abundances for GSE (golden squares) and Kraken (purple circles). Each panel shows the median abundances as dashed lines. Typical errors are indicated in the top-left corner. Notice that Kraken has a relative dearth of elements that are associated with “delayed” sources (e.g., Eu: NSMs, Fe: Type Ia SNe, Ba: NSMs+AGBs) across all panels, supporting the case for a more efficient, shorter star-formation history compared to GSE.

(median: $-1.28^{+0.03}_{-0.03}$). Median abundances are indicated with a dashed line in all panels. We plot and analyze abundances with respect to Mg instead of Fe since Mg has a single production channel (CCSNe) that is tightly coupled to star formation, and thus greatly simplifies our interpretation. We stress again that GSE and Kraken have similar stellar and halo masses, so they make for a controlled setting to reveal the effects of differing star-formation durations (≈ 2 Gyr vs. 3.6 Gyr) on chemical evolution.

The key empirical result of this paper is highlighted in the left panel of Figure 3 – at similar $[\text{Mg}/\text{H}]$, GSE has an elevated $\langle [\text{Eu}/\text{Mg}] \rangle$ compared to Kraken by ≈ 0.3 dex (median $[\text{Eu}/\text{Mg}]$ of $0.22^{+0.10}_{-0.02}$ and $-0.07^{+0.06}_{-0.04}$ respectively). Mg is exclusively produced by CCSNe and thus closely tracks the star-formation history (SFH), whereas Eu is produced in the *r*-process. Since GSE and Kraken had similar stellar masses, at fixed $[\text{Mg}/\text{H}]$ they were enriched by a similar number of CCSNe. Thus, the only reason for higher $[\text{Eu}/\text{Mg}]$ in GSE is its $\approx 2\times$ longer star-formation duration, which is strong evidence for a delayed channel of Eu production (e.g., NSMs). We note that the $[\text{Eu}/\text{Mg}]$ distribution of GSE we measure is consistent with studies based on the GALAH Survey (Matsuno et al. 2021; Buder et al. 2021) and a study of $[\text{Fe}/\text{H}] < -1.5$ GSE stars (Aguado et al. 2020).

Eu is almost exclusively produced via the *r*-process, which may have two channels – an instant channel that tracks the star-formation linked to rCCSNe and a delayed channel due to NSMs. At fixed $[\text{Mg}/\text{H}]$, the number of CCSNe (and rCCSNe) is controlled for, and so a significantly higher $[\text{Eu}/\text{Mg}]$ in GSE implies it has been enriched to a far greater extent by NSMs. This striking difference due to NSMs across ≈ 2 Gyr (Kraken) and 3.6 Gyr (GSE) star-formation durations is strong evidence that enrichment from rCCSNe+NSMs is still evolving > 2 Gyrs after the onset of star-formation in these systems. The magnitude and speed of this evolution provide strong constraints on proposed channels of the *r*-process that we explore in §6.

The panels in Figure 3 depicting a higher $[\text{Fe}/\text{Mg}]$ and $[\text{Ba}/\text{Mg}]$ at fixed $[\text{Mg}/\text{H}]$ further support the overall picture that GSE had a more extended, less efficient star-formation history compared to Kraken. GSE is more enriched in elements that are expected to arise from delayed channels (e.g., Ba from asymptotic giant branch stars (AGBs) & NSMs, Fe from Type Ia SNe) for a similar number of CCSNe as Kraken.

In the final panel of Figure 3 we show $[\text{Eu}/\text{Ba}]$, which is used as a measure of the relative contributions from the *r*-process and s-process, the dominant production pathways for Eu and Ba respectively. For pure *r*-process enrichment, the expected $[\text{Eu}/\text{Ba}]$ is ≈ 0.7 (Snedden et al. 2008). More than half the GSE sample lies close to this limit, whereas Kraken stars have lower $[\text{Eu}/\text{Ba}]$ and span a wider range (≈ -0.1 to ≈ 0.4). The *r*-process in GSE is prolific enough to propel stars closer to the “pure” *r*-

process limit. In what follows we focus on $[\text{Eu}/\text{Mg}]$, and defer the analysis of the remaining abundances (e.g., Ba) that are of great interest for a variety of issues pertaining to chemical evolution to future work.

6. INTERPRETING $[\text{Eu}/\text{Mg}]$ WITH SIMPLE CHEMICAL EVOLUTION MODELS

Because we have good estimates for the star-formation durations of GSE and Kraken (§4), it should be possible to infer a typical timescale for the delayed *r*-process production. To illustrate the power of galaxies with different formation timescales but same final mass, here we produce simple models to translate the difference in $[\text{Eu}/\text{Mg}]$ to constraints on the *r*-process production channels. We emphasize that these models are meant to give an illustrative understanding of the key factors at play, but more complex models will be needed for quantitative constraints using these abundances (e.g., Molero et al. 2021).

6.1. Setup

We model NSMs that result from a star-formation episode with a delay time distribution (DTD, $t_{\text{delay}} \propto t^{-1}$) – no NSMs occur before the minimum delay time (t_{min}). This choice is motivated by theoretical population synthesis results (e.g., Neijssel et al. 2019) and observations that suggest short gamma ray bursts (likely tracing NSMs) follow a DTD of the same shape as Type Ia supernovae (e.g., Paterson et al. 2020). The Eu yield of NSMs is fixed to $M_{\text{Eu}} = 10^{-4.5} M_{\odot}$ per NSM, inferred from the Eu-enhanced ultra-faint dwarfs (Ji et al. 2016a) and consistent with GW170817 (Côté et al. 2018).

For CCSNe and rCCSNe we assume Eu and Mg production occur simultaneously, immediately after a starburst. We adopt a Kroupa (2001) initial mass function with a cutoff of $300 M_{\odot}$ and assume every star $> 10 M_{\odot}$ ends its life as a CCSNe. The effective Eu yield averaged over all CCSNe ($[\text{Eu}/\text{Mg}]_{\text{CCSNe}}$) is left as a free parameter and assumed to be unchanging with time (i.e., the fraction and yield of rCCSNe relative to CCSNe is fixed). The relative rate, $\log(R_{\text{CCSNe}}/R_{\text{NSMs}})$, is allowed to vary from 2-4 based on estimates for NSMs from gravitational wave observations ($286^{+510}_{-237} \text{ Gpc}^{-3} \text{ yr}^{-1}$, The LIGO Scientific Collaboration et al. 2021) and for CCSNe from transient surveys ($1.01^{+0.50}_{-0.35} \times 10^5 \text{ Gpc}^{-3} \text{ yr}^{-1}$, Perley et al. 2020). Note that these are *local* estimates, whereas for Kraken and GSE the $z > 2$ rates are of interest – however, our wide adopted range on the rates likely encompasses the mild evolution expected with redshift (e.g., Neijssel et al. 2019; Santoliquido et al. 2021).

We set the GSE and Kraken star-formation histories to be constant in time (“top-hat”) motivated by the observed GSE age distribution (Bonaca et al. 2020). We assume instant mixing such that enriched gas is converted to stars with no delay – in practice we expect inhomogenous mixing to produce scatter in abundances around the mean trends we predict. With these ingre-

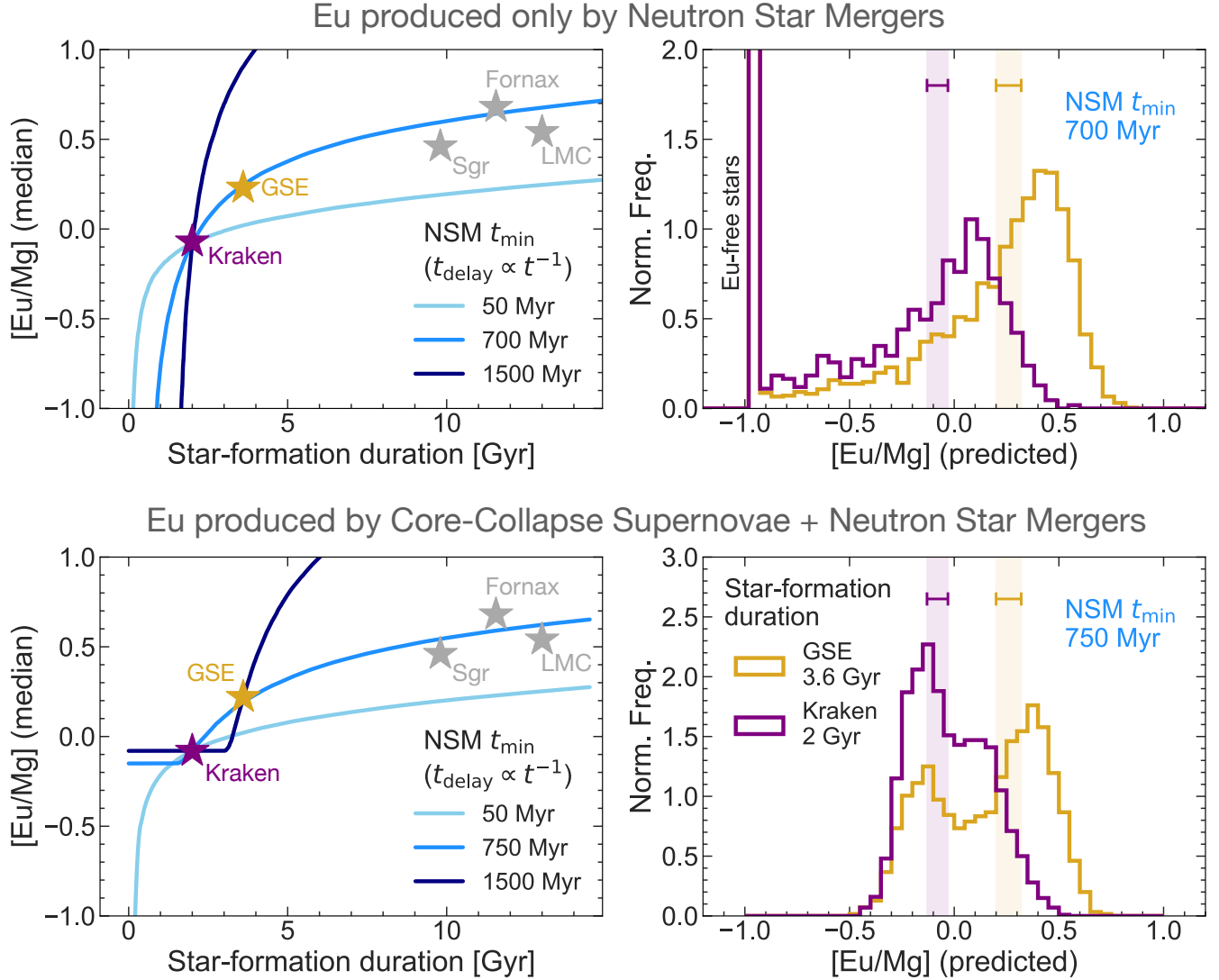


Figure 4. Simple models for the evolution of $[\text{Eu}/\text{Mg}]$. Each track shown in blue is constrained to pass through the Kraken point (purple star) by adjusting $R_{\text{CCSNe}}/R_{\text{NSMs}}$ and the $[\text{Eu}/\text{Mg}]_{\text{CCSNe}}$. On these tracks every point corresponds to an $M_{\star} = 5 \times 10^8 M_{\odot}$ galaxy. The predicted $[\text{Eu}/\text{Mg}]$ distributions shown on the right include a 0.1 dex uncertainty for comparison with observations. The median $[\text{Eu}/\text{Mg}]$ we measure is shown as shaded regions, and all Eu-free stars are set to $[\text{Eu}/\text{Mg}] = -1$. Statistical errors on the median $[\text{Eu}/\text{Mg}]$ for all galaxies shown in the left panels are smaller than the star-shaped markers used to represent them. **Top:** Models where Eu arises purely from NSMs require minimum delay times $\approx 500 - 1000$ Myrs to match the rapid evolution across Kraken and GSE (top-left). Such delay times imply the existence of substantial fractions of Eu-free stars inconsistent with observations (top-right). **Bottom:** When contributions from both CCSNe and NSMs are allowed, there is a “floor” for $[\text{Eu}/\text{Mg}]$ at early times due to CCSNe followed by a rapid rise from delayed NSMs. Models with $t_{\min} \approx 500 - 1000$ Myrs reproduce the abundances in Kraken and GSE as well as in dwarfs with extended star-formation histories (Sgr, LMC, Fornax). The predicted $[\text{Eu}/\text{Mg}]$ distribution (right panel) is bimodal, with each mode corresponding to the CCSNe phase and NSM plateau phase of the tracks.

dients we are able to produce tracks of $[\text{Eu}/\text{Mg}]$ as a function of star-formation duration. Our simple models are able to perfectly reproduce the more sophisticated $[\text{Eu}/\text{Mg}]$ chemical evolution model for GSE by [Matsumo et al. \(2021\)](#).

In addition to the $[\text{Eu}/\text{Mg}]$ data we have measured for Kraken and GSE, we also compare our models qualitatively against $[\text{Eu}/\text{Mg}]$ measured for dwarf galaxies of comparable mass (LMC, Fornax, and Sgr). For the LMC we draw on [Van der Swaelmen et al. \(2013\)](#) who measured $[\text{Eu}/\text{Mg}]$ for 94 stars spanning $[\text{Fe}/\text{H}]$ of -0.9 to -0.4 (10^{th} and 90^{th} percentiles, median $[\text{Fe}/\text{H}]$ of $-0.66^{+0.02}_{-0.02}$). The $[\text{Eu}/\text{Mg}]$ for Fornax is from [Letarte et al. \(2018\)](#), who present $[\text{Eu}/\text{Mg}]$ for 70 stars with $[\text{Fe}/\text{H}]$ spanning -1.5 to -0.6 (median $[\text{Fe}/\text{H}]$ of $-0.86^{+0.02}_{-0.01}$). For Sgr, we rely on [Bonifacio et al. \(2000\)](#); [McWilliam et al. \(2013\)](#) who measured these abundances for five stars spanning $[\text{Fe}/\text{H}]$ of -0.1 and -0.5 . Star-formation durations for these galaxies (all $\gtrsim 10$ Gyrs) are sourced from [Weisz et al. \(2014\)](#) – in particular, we adopt their t_{90} which is the time taken to form 90% of the stellar mass. These galaxies do not have simple top-hat star-formation histories, their abundances are measured on different scales, and $[\text{Eu}/\text{Mg}]$ is measured mostly at the metal-rich end of these galaxies, i.e., they are probing the $[\text{Eu}/\text{Mg}]$ at the very end of the SFH and not the median $[\text{Eu}/\text{Mg}]$ across the entire SFH. For these reasons we do not make detailed quantitative comparisons, but nonetheless plot these data as indicative of the long-run “plateau” $[\text{Eu}/\text{Mg}]$ in galaxies with extended star-formation histories.

6.2. Model I: only rCCSNe produce Eu

The first model we briefly consider assumes Eu is produced solely by rCCSNe. Such a model is already disfavored based on Figure 3, since GSE shows higher $[\text{Eu}/\text{Mg}]$ than Kraken at similar $[\text{Mg}/\text{H}]$ (i.e., similar number of CCSNe and rCCSNe). As per our setup, rCCSNe produce flat tracks in $[\text{Eu}/\text{Mg}]$ as a function of star-formation duration since both Eu and Mg are produced in similar proportions over time. For a significant difference in $[\text{Eu}/\text{Mg}]$ to emerge across Kraken and GSE time-dependent/delayed sources that increase Eu production with time are necessary.

6.3. Model II: only NSMs produce Eu

In this model we assume NSMs are solely responsible for all Eu production. When NSMs are the only r -process channel, t_{min} (the minimum delay time) is the key parameter that sets the relative $[\text{Eu}/\text{Mg}]$. We show tracks spanning a range of t_{min} in the top-left panel of Figure 4 constrained to match the Kraken value. Short t_{min} (e.g., 10-50 Myr) result in rapidly plateauing $[\text{Eu}/\text{Mg}]$ at odds with the data. We find $t_{\text{min}} = 611^{+147}_{-151}$ Myrs by adopting a uniform prior between 0-3.6 Gyr and maximizing the likelihood such that there is a dif-

ference in median $[\text{Eu}/\text{Mg}]$ of 0.30 ± 0.05 dex across the Kraken and GSE SF durations.

However, a > 500 Myr delay time implies the existence of substantial fractions of Eu-free stars that formed prior to the onset of NSMs (top-right, Figure 4). At least $\approx 25\%$ of the stars in Kraken and $\approx 15\%$ of the stars in GSE would be Eu-free. We do not observe any Eu-free stars. For GSE this might be because our sample does not extend below $[\text{Fe}/\text{H}] < -1.5$ to probe ages $\lesssim 500$ Myr ($\approx 15\%$ of the SFH). Though [Aguado et al. \(2020\)](#) find Eu detections ($[\text{Eu}/\text{Mg}] \approx 0$) in all four GSE stars they studied with $[\text{Fe}/\text{H}]$ of -1.4 to -1.8 . More strikingly, in Kraken, for which half our sample is at $[\text{Fe}/\text{H}] < -1.5$, we detect Eu in every star, including in stars as metal-poor as $[\text{Fe}/\text{H}] = -2.0$. Note that assuming a steeper delay time distribution ($t_{\text{delay}} \propto t^{-1.5}$, e.g., [Côté et al. 2019](#)) only makes matters worse by favoring longer t_{min} as the $[\text{Eu}/\text{Mg}]$ plateau occurs even more rapidly. On the other hand a much shallower $t_{\text{delay}} \propto t^{+0.5}$ ([Tsujimoto 2021](#)) produces a gently rising $[\text{Eu}/\text{Mg}]$, with no Eu-free stars, but is disfavored by NSM models⁴ (e.g., [Chruslinska et al. 2018](#); [Belczynski et al. 2018](#); [Neijssel et al. 2019](#)).

6.4. Model III: rCCSNe+NSMs produce Eu

In this model we assume Eu arises from rCCSNe as well as NSMs. The dearth of Eu-free stars that emerges from Model II can be explained by contributions from early rCCSNe. rCCSNe produce Eu promptly after star-formation, and therefore ensure a floor for $[\text{Eu}/\text{Mg}]$ at early times. Once the NSMs begin contributing after the minimum delay time, t_{min} , the $[\text{Eu}/\text{Mg}]$ begins rising.

For a floor of $[\text{Eu}/\text{Mg}] \gtrsim -0.25$ suggested by the Kraken distribution in Figure 3, we find only models with $t_{\text{delay}} \gtrsim 500$ Myr are able to match the evolution across Kraken and GSE (bottom row, Figure 4). Requiring a plateau value of $[\text{Eu}/\text{Mg}] \approx 0.5$ for ≈ 10 Gyr star-formation durations observed in galaxies of comparable mass – Sagittarius, Fornax, and the Large Magellanic Cloud – provides an upper bound of $t_{\text{delay}} \lesssim 1000$ Myr (see navy blue curve in bottom-left panel of Figure 4). The predicted $[\text{Eu}/\text{Mg}]$ distributions for GSE and Kraken are consistent with the data at hand – the distributions are bimodal, with one mode corresponding to the rCCSNe-only phase and the other close to the peak $[\text{Eu}/\text{Mg}]$ reached during the rCCSNe+NSM phase.

⁴ In detail, [Tsujimoto \(2021\)](#) are effectively fitting the *enrichment* DTD as $t_{\text{delay}} \propto t^{+0.5}$ and not the *merger* DTD. See §7.2 for discussion of the distinction. Accounting for this, our findings are in excellent qualitative agreement (i.e., NSMs+rCCSNe are required, NSMs must produce delayed enrichment).

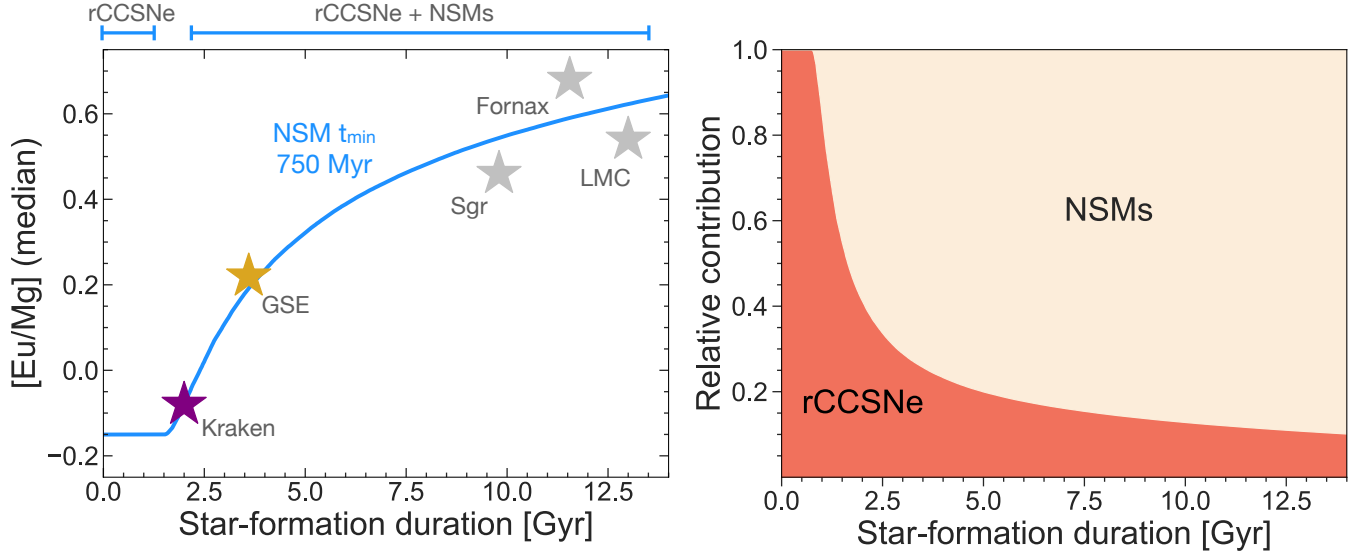


Figure 5. **Left:** Schematic of our preferred scenario featuring both rare CCSNe and NSMs with a $t_{\min} = 750$ Myr. Only systems with stellar masses comparable to Kraken and GSE are shown for fair comparison. **Right:** The relative contribution of rCCSNe and NSMs to the total Eu produced as a function of star-formation duration. rCCSNe contribute significantly at early times in galaxies like Kraken ($\approx 50\%$ of Eu), whereas in galaxies like Sgr and Fornax $\approx 85\%$ of Eu arises from NSMs.

7. DISCUSSION

7.1. A role for both rCCSNe and NSMs

Our models show both rCCSNe and NSMs have a role to play in r -process enrichment – rCCSNe dominate at early times ($\lesssim 2$ Gyr), while NSMs take over at later epochs (Figure 5). Without delayed enrichment from NSMs, the sharp rise in [Eu/Mg] with star-formation duration is not possible, and without rCCSNe a large population of Eu-free stars would be produced at early times. For our fiducial model shown in the left-panel of Figure 5, $\approx 50\%$ of all Eu produced in Kraken arises from rCCSNe. However, for longer star-formation durations (e.g., in Sgr), NSMs dominate and account for $\approx 85\%$ of the Eu. Note that the yield of individual rCCSNe (e.g., collapsars) producing Eu could be much higher than NSMs (e.g., Siegel et al. 2019) but the effective yield averaged over all CCSNe (i.e., accounting for the rarity of rCCSNe) is lower than NSMs (see right panel of Figure 5).

The idea that both rCCSNe and NSMs are required to explain r -process in galaxies ranging from the MW to dwarf galaxies is not new. Several recent models have used both sites to successfully reproduce r -process chemical evolution in the MW, especially if CCSNe stop producing r -process at higher metallicities (e.g., Ting et al. 2012; Matteucci et al. 2014; Cescutti et al. 2015; Wehmeyer et al. 2015; Haynes & Kobayashi 2019; Côté et al. 2019; Siegel et al. 2019). The latter is expected in currently viable r -process mechanisms for rCCSNe, because high angular momentum is needed to create jets or accretion disks (e.g., Mösta et al. 2018; Siegel et al. 2019) and metal-rich stars lose a larger fraction of their angu-

lar momentum to winds. It also appears likely that both rCCSNe and NSMs are needed to explain Eu evolution of intact dwarf galaxies with M_{\star} ranging from 10^4 – $8 M_{\odot}$ (e.g., Ji et al. 2016b; Skúladóttir et al. 2019; Molero et al. 2021; de los Reyes et al. 2021). However, we note that all chemical evolution models, including our simple models here, can only show that the combination of rCCSNe and NSMs is sufficient, but not necessary, to explain the data. The crucial uncertainty is whether very prompt NSMs ($\lesssim 10$ Myrs) that are able to enrich star-forming regions are sufficiently common because these NSMs would effectively mimic rCCSNe from a chemical evolution standpoint (e.g., Beniamini & Piran 2019; Safarzadeh et al. 2019; Simonetti et al. 2019; Andrews et al. 2020; Romero-Shaw et al. 2020; Kirby et al. 2020). However, there is some evidence against fast mergers being a dominant population from short gamma ray burst redshift distributions and host galaxy populations (e.g., Côté et al. 2019; Simonetti et al. 2019), so the most likely scenario appears to be that both rCCSNe and NSMs are required.

7.2. Natal kicks and cooling times may explain the $\approx 500 - 1000$ Myr delay time for enrichment from NSMs

At face value, our models suggest a minimum delay time, $t_{\min} \approx 500 - 1000$ Myr for NSMs, seemingly at odds with the vast majority of theoretical binary evolution models that predict t_{\min} on the order of $\approx 10 - 30$ Myrs (e.g., Chruslinska et al. 2018; Belczynski et al. 2018; Neijssel et al. 2019). However, our inferred t_{\min} not only includes the time it takes for neutron stars to merge, but also the time required for the produced ele-

ments to find their way into subsequent generations of stars. That is, the delay time for mergers, and the delay time for *enrichment* from mergers could be substantially different.

This substantial difference – a $\approx 10 - 30$ Myr delay time for mergers, but a $500 - 1000$ Myr delay for *r*-process enrichment due to NSMs – may be explained by considering natal kicks (velocity impulses from supernova explosions) from NSMs. Due to both these mechanisms, NSMs potentially enrich gas far from active star-forming regions of their hosts, thus altering patterns of *r*-process enrichment (Bramante & Linden 2016; Macias & Ramirez-Ruiz 2019; Banerjee et al. 2020; van de Voort et al. 2021). Natal kicks propel neutron stars off the disk – short GRBs (likely tracing NSMs) are observed at typical distances of $\approx 1.5 \times$ half-light radii, and often off the plane, in $10^{8.5} - 10^{11.5} M_{\odot}$ galaxies (e.g., Fong & Berger 2013). This effect is likely more pronounced in $z \gtrsim 2$ systems like GSE and Kraken, whose disks are thick, turbulent, and have relatively lower binding energies versus the more settled disks seen in local, $z \approx 0$ systems (e.g., Bird et al. 2013; Ma et al. 2017; Park et al. 2020).

Due to both these effects, the NSMs in GSE and Kraken may have merged with $t_{\min} \approx 10 - 30$ Myrs, but may have ended up enriching gas outside the interstellar medium (ISM) that was yet to cool into a star-forming state⁵. The expected cooling/condensation time for extra-planar gas at $\approx 1 - 2r_e$ for Kraken and GSE-like galaxies at $z \approx 2 - 3$ is expected to be on the order of few hundred Myrs to a Gyr (Eqn. 12 of Fraternali 2017, Eqns. 8.94-8.95 of Mo et al. 2010; GSE physical parameters from Naidu et al. 2021), comparable to the dynamical time of the halos. Thus, the cooling time may entirely account for the high t_{\min} we infer.

The implication is that metal poor stars that probe the first few hundred Myrs of star-formation in a variety of systems, and that are widely analyzed to understand the *r*-process may be exclusively sampling yields from rCCSNe since the *r*-process enriched gas is yet to rain down and form stars. This also explains why galaxies like Sculptor, Sagittarius, and Fornax have relatively flat $[\text{Eu}/\text{Mg}] \approx -0.1$ to 0.0 sequences as a function of $[\text{Fe}/\text{H}]$ and age (Skúladóttir & Salvadori 2020), during the first few Gyrs of their star-formation history when rCCSNe ostensibly account for their *r*-enrichment (right panel of Figure 5).

7.3. Caveats & Outlook

A persisting puzzle entirely independent of the results presented here is why the MW has a gently evolving

$[\text{Eu}/\text{Mg}] \approx 0.0 - 0.1$ for stars that formed $0 - 10$ Gyrs ago, and a virtually flat track in $[\text{Eu}/\text{Mg}]$ vs. $[\text{Fe}/\text{H}]$ with almost no stars reaching $[\text{Eu}/\text{Mg}] \approx 0.5$ (Skúladóttir & Salvadori 2020). Galaxies like the LMC, Fornax, and Sgr have much higher $[\text{Eu}/\text{Mg}]$ at fixed metallicity compared to the MW. Our simple rCCSNe+NSM model (Figure 5) explains the $[\text{Eu}/\text{Mg}]$ evolution in these galaxies, but not in the MW. Sophisticated models that account for the MW’s rich merger history, complex SFH, differential mixing, and inside-out growth are required to understand the Galactic $[\text{Eu}/\text{Mg}]$ evolution.

We emphasize once again that our simple analytical models are meant to give a broad, qualitative sense for the situation. There are additional complexities that are well-motivated, but poorly empirically constrained, that we do not explore here – e.g., metallicity-dependent *r*-process yields, deviations from simple t^{-1} DTDs, departures from the instant enrichment assumption.

We adopted a star-formation duration of 2 Gyrs for Kraken based on Kruijssen et al. (2020), but the conservative range for this quantity is $\approx 1.5 - 3.6$ Gyrs (§4). Age distributions from Kraken’s MSTO stars and self-consistent age determinations for the entire sample of Kraken GCs (only half have published ages) will tighten this range, and also test the validity of our top-hat star-formation history assumption. For now, we note that > 2 Gyr (< 2 Gyr) star-formation durations produce longer (shorter) t_{\min} for enrichment from NSMs that are still $\approx 10 - 100 \times$ larger than the $t_{\min} \approx 10 - 30$ Myr expected from theory. For instance, a > 1.5 Gyr star-formation duration for Kraken results in a > 300 Myr delay for Models II and III.

Future observations can further test our proposed picture by analyzing additional disrupted dwarfs. Of particular interest are systems like I’itoi (Naidu et al. 2020) and Thamnos (Koppelman et al. 2019) which may have star-formation durations even shorter than Kraken and may thus directly constrain the pure Eu yield of rCCSNe. For Kraken and GSE themselves, abundances for larger samples spanning the entirety of their star-formation histories will enable detailed comparisons against the predicted bimodal $[\text{Eu}/\text{Mg}]$ distributions from our preferred model. Confirming the existence and location of these modes will yield rich insights.

The convenient, star-by-star access to “high- z ” galaxies afforded by the disrupted dwarfs within a few kpc from the Sun is set to transform our understanding of early Universe chemistry as more of these systems are unearthed and characterized. This work provides a glimpse of the unique constraints that might be possible with dozens of such systems in the imminent future.

Facilities: Magellan (MIKE), *Gaia*

Software: IPython (Pérez & Granger 2007), matplotlib (Hunter 2007), numpy (Oliphant 2006--), scipy (Virtanen et al. 2020), jupyter (Kluyver et al. 2016), gala (Price-Whelan

⁵ Schönrich & Weinberg (2019) considered a multi-phase ISM for the MW and found the opposite conclusion, that NSMs would have to rapidly enrich cold ISM instead of hot ISM; however, they only considered *r*-process production in NSMs without CCSNe.

2017; Price-Whelan et al. 2017), Astropy (Astropy Collaboration et al. 2013, 2018), smhr (Casey 2014), CarPy (Kelson 2003), MOOG (Snedden 1973; Sobeck et al. 2011)

ACKNOWLEDGMENTS

We thank ace Magellan observer Yuri Beletsky for collecting these data for us amidst the vicissitudes of a pandemic. We are grateful to the CfA and U. Chicago TACs for their continued support of this long-term project. We thank Tadafumi Matsuno and Yutaka Hirai for sharing their GSE chemical evolution tracks from Matsuno et al. (2021) that gave us great confidence in our elementary models. We thank Anna-Christina Eilers for sharing an updated version of the Hogg et al. (2019); Eilers et al. (2019) catalog with us. This project was inspired by a renegade meeting on the sidelines of EAS 2021 whose ringleaders were Ana Bonaca, Chervin Laporte, and Diederik Kruijssen. We acknowledge illuminating conversations with Aaron Dotter and Seth Gosage on the Kraken globular clusters, the kindness of Holger Baumgardt in helping compile their CMDs, and the generosity of Christian Johnson for discussing the many mysteries of NGC 6273. We had the fortune of discussing NSM kicks with Freeke van de Voort. RPN thanks Michelle Peters for her infinite kindness on post-observing days.

RPN acknowledges an Ashford Fellowship granted by Harvard University. CC acknowledges funding from the Packard foundation. YST acknowledges financial support from the Australian Research Council through DECRA Fellowship DE220101520.

This work has made use of data from the European Space Agency (ESA) mission *Gaia* (<https://www.cosmos.esa.int/gaia>), processed by the *Gaia* Data Processing and Analysis Consortium (DPAC, <https://www.cosmos.esa.int/web/gaia/dpac/consortium>) (Gaia Collaboration et al. 2016, 2021). Funding for the DPAC has been provided by national institutions, in particular the institutions participating in the *Gaia* Multilateral Agreement.

Funding for the Sloan Digital Sky Survey IV has been provided by the Alfred P. Sloan Foundation, the U.S. Department of Energy Office of Science, and the Participating Institutions. SDSS-IV acknowledges support and resources from the Center for High Performance Computing at the University of Utah. The SDSS website is www.sdss.org. SDSS-IV is managed by the Astrophysical Research Consortium for the Participating Institutions of the SDSS Collaboration including the Brazilian Participation Group, the Carnegie Institution for Science, Carnegie Mellon University, Center for Astrophysics — Harvard & Smithsonian, the Chilean Participation Group, the French Participation Group, Instituto de Astrofísica de Canarias, The Johns Hopkins University, Kavli Institute for the Physics and Mathematics of the Universe (IPMU) / University of Tokyo, the Korean Participation Group, Lawrence Berkeley National Laboratory, Leibniz Institut für Astrophysik Potsdam (AIP), Max-Planck-Institut für Astronomie (MPIA Heidelberg), Max-Planck-Institut für Astrophysik (MPA Garching), Max-Planck-Institut für Extraterrestrische Physik (MPE), National Astronomical Observatories of China, New Mexico State University, New York University, University of Notre Dame, Observatório Nacional / MCTI, The Ohio State University, Pennsylvania State University, Shanghai Astronomical Observatory, United Kingdom Participation Group, Universidad

REFERENCES

- Aguado, D. S., Belokurov, V., Myeong, G. C., et al. 2020, arXiv e-prints, arXiv:2012.01430. <https://arxiv.org/abs/2012.01430>
- Amorisco, N. C. 2017, MNRAS, 464, 2882, doi: [10.1093/mnras/stw2229](https://doi.org/10.1093/mnras/stw2229)
- Andrews, J. J., Breivik, K., Pankow, C., D’Orazio, D. J., & Safarzadeh, M. 2020, ApJL, 892, L9, doi: [10.3847/2041-8213/ab5b9a](https://doi.org/10.3847/2041-8213/ab5b9a)
- Astropy Collaboration, Robitaille, T. P., Tollerud, E. J., et al. 2013, A&A, 558, A33, doi: [10.1051/0004-6361/201322068](https://doi.org/10.1051/0004-6361/201322068)
- Astropy Collaboration, Price-Whelan, A. M., Sipőcz, B. M., et al. 2018, AJ, 156, 123, doi: [10.3847/1538-3881/aabc4f](https://doi.org/10.3847/1538-3881/aabc4f)
- Banerjee, P., Wu, M.-R., & Yuan, Z. 2020, ApJL, 902, L34, doi: [10.3847/2041-8213/abbc0d](https://doi.org/10.3847/2041-8213/abbc0d)
- Barklem, P. S., Piskunov, N., & O’Mara, B. J. 2000, A&AS, 142, 467, doi: [10.1051/aas:2000167](https://doi.org/10.1051/aas:2000167)
- Baumgardt, H., & Hilker, M. 2018, MNRAS, 478, 1520, doi: [10.1093/mnras/sty1057](https://doi.org/10.1093/mnras/sty1057)
- Baumgardt, H., Hilker, M., Sollima, A., & Bellini, A. 2019, MNRAS, 482, 5138, doi: [10.1093/mnras/sty2997](https://doi.org/10.1093/mnras/sty2997)
- Belczynski, K., Askar, A., Arca-Sedda, M., et al. 2018, A&A, 615, A91, doi: [10.1051/0004-6361/201732428](https://doi.org/10.1051/0004-6361/201732428)
- Belokurov, V., Erkal, D., Evans, N. W., Koposov, S. E., & Deason, A. J. 2018, MNRAS, 478, 611, doi: [10.1093/mnras/sty982](https://doi.org/10.1093/mnras/sty982)
- Belokurov, V., Sanders, J. L., Fattahi, A., et al. 2020, MNRAS, 494, 3880, doi: [10.1093/mnras/staa876](https://doi.org/10.1093/mnras/staa876)
- Beniamini, P., & Piran, T. 2019, MNRAS, 487, 4847, doi: [10.1093/mnras/stz1589](https://doi.org/10.1093/mnras/stz1589)
- Bernstein, R., Sackett, S. A., Gunnels, S. M., Mochnacki, S., & Athey, A. E. 2003, Proc. SPIE, 4841, 1694, doi: [10.1117/12.461502](https://doi.org/10.1117/12.461502)
- Bird, J. C., Kazantzidis, S., Weinberg, D. H., et al. 2013, ApJ, 773, 43, doi: [10.1088/0004-637X/773/1/43](https://doi.org/10.1088/0004-637X/773/1/43)
- Bird, S. A., Xue, X.-X., Liu, C., et al. 2019, AJ, 157, 104, doi: [10.3847/1538-3881/aaf2de](https://doi.org/10.3847/1538-3881/aaf2de)
- Bonaca, A., Conroy, C., Cargile, P. A., et al. 2020, ApJL, 897, L18, doi: [10.3847/2041-8213/ab9caa](https://doi.org/10.3847/2041-8213/ab9caa)
- Bonifacio, P., Monai, S., & Beers, T. C. 2000, AJ, 120, 2065, doi: [10.1086/301566](https://doi.org/10.1086/301566)
- Bramante, J., & Linden, T. 2016, ApJ, 826, 57, doi: [10.3847/0004-637X/826/1/57](https://doi.org/10.3847/0004-637X/826/1/57)
- Buder, S., Lind, K., Ness, M. K., et al. 2021, arXiv e-prints, arXiv:2109.04059. <https://arxiv.org/abs/2109.04059>
- Casey, A. R. 2014, PhD thesis, Australian National University
- Castelli, F., & Kurucz, R. L. 2004, ArXiv Astrophysics e-prints
- Cescutti, G., Romano, D., Matteucci, F., Chiappini, C., & Hirschi, R. 2015, A&A, 577, A139, doi: [10.1051/0004-6361/201525698](https://doi.org/10.1051/0004-6361/201525698)
- Chruslinska, M., Belczynski, K., Klencki, J., & Benacquista, M. 2018, MNRAS, 474, 2937, doi: [10.1093/mnras/stx2923](https://doi.org/10.1093/mnras/stx2923)
- Conroy, C., Naidu, R. P., Zaritsky, D., et al. 2019, ApJ, 887, 237, doi: [10.3847/1538-4357/ab5710](https://doi.org/10.3847/1538-4357/ab5710)
- Côté, B., Fryer, C. L., Belczynski, K., et al. 2018, ApJ, 855, 99, doi: [10.3847/1538-4357/aaad67](https://doi.org/10.3847/1538-4357/aaad67)
- Côté, B., Eichler, M., Arcones, A., et al. 2019, ApJ, 875, 106, doi: [10.3847/1538-4357/ab10db](https://doi.org/10.3847/1538-4357/ab10db)
- Cowan, J. J., Sneden, C., Lawler, J. E., et al. 2021, Reviews of Modern Physics, 93, 015002, doi: [10.1103/RevModPhys.93.015002](https://doi.org/10.1103/RevModPhys.93.015002)
- Das, P., Hawkins, K., & Jofré, P. 2020, MNRAS, 493, 5195, doi: [10.1093/mnras/stz3537](https://doi.org/10.1093/mnras/stz3537)
- de los Reyes, M. A. C., Kirby, E. N., Ji, A. P., & Nuñez, E. H. 2021, arXiv e-prints, arXiv:2110.01690. <https://arxiv.org/abs/2110.01690>
- Dotter, A., Sarajedini, A., & Anderson, J. 2011, ApJ, 738, 74, doi: [10.1088/0004-637X/738/1/74](https://doi.org/10.1088/0004-637X/738/1/74)
- Dotter, A., Sarajedini, A., Anderson, J., et al. 2010, ApJ, 708, 698, doi: [10.1088/0004-637X/708/1/698](https://doi.org/10.1088/0004-637X/708/1/698)
- Drout, M. R., Piro, A. L., Shappee, B. J., et al. 2017, Science, 358, 1570, doi: [10.1126/science.aag0049](https://doi.org/10.1126/science.aag0049)
- Duggan, G. E., Kirby, E. N., Andrievsky, S. M., & Korotin, S. A. 2018, ApJ, 869, 50, doi: [10.3847/1538-4357/aab8e](https://doi.org/10.3847/1538-4357/aab8e)
- Eilers, A.-C., Hogg, D. W., Rix, H.-W., & Ness, M. K. 2019, ApJ, 871, 120, doi: [10.3847/1538-4357/aaf648](https://doi.org/10.3847/1538-4357/aaf648)
- Fernández-Alvar, E., Carigi, L., Schuster, W. J., et al. 2018, ApJ, 852, 50, doi: [10.3847/1538-4357/aa9ced](https://doi.org/10.3847/1538-4357/aa9ced)
- Fong, W., & Berger, E. 2013, ApJ, 776, 18, doi: [10.1088/0004-637X/776/1/18](https://doi.org/10.1088/0004-637X/776/1/18)
- Forbes, D. A. 2020, MNRAS, 493, 847, doi: [10.1093/mnras/staa245](https://doi.org/10.1093/mnras/staa245)
- Forsberg, R., Jönsson, H., Ryde, N., & Matteucci, F. 2019, A&A, 631, A113, doi: [10.1051/0004-6361/201936343](https://doi.org/10.1051/0004-6361/201936343)
- Fraternali, F. 2017, in Astrophysics and Space Science Library, Vol. 430, Gas Accretion onto Galaxies, ed. A. Fox & R. Davé, 323, doi: [10.1007/978-3-319-52512-9_14](https://doi.org/10.1007/978-3-319-52512-9_14)
- Gaia Collaboration, Prusti, T., de Bruijne, J. H. J., et al. 2016, A&A, 595, A1, doi: [10.1051/0004-6361/201629272](https://doi.org/10.1051/0004-6361/201629272)
- Gaia Collaboration, Brown, A. G. A., Vallenari, A., et al. 2021, A&A, 649, A1, doi: [10.1051/0004-6361/202039657](https://doi.org/10.1051/0004-6361/202039657)
- Gallart, C., Bernard, E. J., Brook, C. B., et al. 2019, Nature Astronomy, 3, 932, doi: [10.1038/s41550-019-0829-5](https://doi.org/10.1038/s41550-019-0829-5)
- Halevi, G., & Mösta, P. 2018, MNRAS, 477, 2366, doi: [10.1093/mnras/sty797](https://doi.org/10.1093/mnras/sty797)

- Hawkins, K., Jofré, P., Masseron, T., & Gilmore, G. 2015, MNRAS, 453, 758, doi: [10.1093/mnras/stv1586](https://doi.org/10.1093/mnras/stv1586)
- Haynes, C. J., & Kobayashi, C. 2019, MNRAS, 483, 5123, doi: [10.1093/mnras/sty3389](https://doi.org/10.1093/mnras/sty3389)
- Helmi, A., Babusiaux, C., Koppelman, H. H., et al. 2018, Nature, 563, 85, doi: [10.1038/s41586-018-0625-x](https://doi.org/10.1038/s41586-018-0625-x)
- Hogg, D. W., Eilers, A.-C., & Rix, H.-W. 2019, AJ, 158, 147, doi: [10.3847/1538-3881/ab398c](https://doi.org/10.3847/1538-3881/ab398c)
- Horta, D., Schiavon, R. P., Mackereth, J. T., et al. 2021, MNRAS, 500, 1385, doi: [10.1093/mnras/staa2987](https://doi.org/10.1093/mnras/staa2987)
- Hunter, J. D. 2007, Computing In Science & Engineering, 9, 90, doi: [10.1109/MCSE.2007.55](https://doi.org/10.1109/MCSE.2007.55)
- Ji, A. P., Frebel, A., Chiti, A., & Simon, J. D. 2016a, Nature, 531, 610, doi: [10.1038/nature17425](https://doi.org/10.1038/nature17425)
- Ji, A. P., Frebel, A., Simon, J. D., & Chiti, A. 2016b, ApJ, 830, 93, doi: [10.3847/0004-637X/830/2/93](https://doi.org/10.3847/0004-637X/830/2/93)
- Ji, A. P., Li, T. S., Hansen, T. T., et al. 2020, AJ, 160, 181, doi: [10.3847/1538-3881/abacb6](https://doi.org/10.3847/1538-3881/abacb6)
- Jönsson, H., Ryde, N., Nordlander, T., et al. 2017, A&A, 598, A100, doi: [10.1051/0004-6361/201629128](https://doi.org/10.1051/0004-6361/201629128)
- Jönsson, H., Holtzman, J. A., Allende Prieto, C., et al. 2020, AJ, 160, 120, doi: [10.3847/1538-3881/aba592](https://doi.org/10.3847/1538-3881/aba592)
- Kasen, D., Metzger, B., Barnes, J., Quataert, E., & Ramirez-Ruiz, E. 2017, Nature, 551, 80, doi: [10.1038/nature24453](https://doi.org/10.1038/nature24453)
- Kasliwal, M. M., Nakar, E., Singer, L. P., et al. 2017, Science, 358, 1559, doi: [10.1126/science.aap9455](https://doi.org/10.1126/science.aap9455)
- Kelson, D. D. 2003, PASP, 115, 688, doi: [10.1086/375502](https://doi.org/10.1086/375502)
- Kirby, E. N., Duggan, G., Ramirez-Ruiz, E., & Macias, P. 2020, ApJL, 891, L13, doi: [10.3847/2041-8213/ab78a1](https://doi.org/10.3847/2041-8213/ab78a1)
- Kluyver, T., Ragan-Kelley, B., Pérez, F., et al. 2016, in Positioning and Power in Academic Publishing: Players, Agents and Agendas, ed. F. Loizides & B. Schmidt, IOS Press, 87 – 90
- Kobayashi, C., Karakas, A. I., & Lugaro, M. 2020, ApJ, 900, 179, doi: [10.3847/1538-4357/abae65](https://doi.org/10.3847/1538-4357/abae65)
- Koch, A., Grebel, E. K., Gilmore, G. F., et al. 2008, AJ, 135, 1580, doi: [10.1088/0004-6256/135/4/1580](https://doi.org/10.1088/0004-6256/135/4/1580)
- Koppelman, H. H., Bos, R. O. Y., & Helmi, A. 2020, A&A, 642, L18, doi: [10.1051/0004-6361/202038652](https://doi.org/10.1051/0004-6361/202038652)
- Koppelman, H. H., Helmi, A., Massari, D., Price-Whelan, A. M., & Starkenburg, T. K. 2019, A&A, 631, L9, doi: [10.1051/0004-6361/201936738](https://doi.org/10.1051/0004-6361/201936738)
- Kroupa, P. 2001, MNRAS, 322, 231, doi: [10.1046/j.1365-8711.2001.04022.x](https://doi.org/10.1046/j.1365-8711.2001.04022.x)
- Kruijssen, J. M. D., Pfeffer, J. L., Reina-Campos, M., Crain, R. A., & Bastian, N. 2019, MNRAS, 486, 3180, doi: [10.1093/mnras/sty1609](https://doi.org/10.1093/mnras/sty1609)
- Kruijssen, J. M. D., Pfeffer, J. L., Chevance, M., et al. 2020, arXiv e-prints, arXiv:2003.01119, <https://arxiv.org/abs/2003.01119>
- Letarte, B., Hill, V., Tolstoy, E., et al. 2018, A&A, 613, C1, doi: [10.1051/0004-6361/200913413e](https://doi.org/10.1051/0004-6361/200913413e)
- Leung, H. W., & Bovy, J. 2019, MNRAS, 489, 2079, doi: [10.1093/mnras/stz2245](https://doi.org/10.1093/mnras/stz2245)
- Lomaeva, M., Jönsson, H., Ryde, N., Schultheis, M., & Thorsbro, B. 2019, A&A, 625, A141, doi: [10.1051/0004-6361/201834247](https://doi.org/10.1051/0004-6361/201834247)
- Ma, X., Hopkins, P. F., Faucher-Giguère, C.-A., et al. 2016, MNRAS, 456, 2140, doi: [10.1093/mnras/stv2659](https://doi.org/10.1093/mnras/stv2659)
- Ma, X., Hopkins, P. F., Feldmann, R., et al. 2017, MNRAS, 466, 4780, doi: [10.1093/mnras/stx034](https://doi.org/10.1093/mnras/stx034)
- Macias, P., & Ramirez-Ruiz, E. 2019, ApJL, 877, L24, doi: [10.3847/2041-8213/ab2049](https://doi.org/10.3847/2041-8213/ab2049)
- Mackereth, J. T., & Bovy, J. 2020, MNRAS, 492, 3631, doi: [10.1093/mnras/staa047](https://doi.org/10.1093/mnras/staa047)
- Massari, D., Koppelman, H. H., & Helmi, A. 2019, A&A, 630, L4, doi: [10.1051/0004-6361/201936135](https://doi.org/10.1051/0004-6361/201936135)
- Matsuno, T., Hirai, Y., Tarumi, Y., et al. 2021, arXiv e-prints, arXiv:2101.07791, <https://arxiv.org/abs/2101.07791>
- Matteucci, F., Romano, D., Arcones, A., Korobkin, O., & Rosswog, S. 2014, MNRAS, 438, 2177, doi: [10.1093/mnras/stt2350](https://doi.org/10.1093/mnras/stt2350)
- McWilliam, A., Wallerstein, G., & Mottini, M. 2013, ApJ, 778, 149, doi: [10.1088/0004-637X/778/2/149](https://doi.org/10.1088/0004-637X/778/2/149)
- Mo, H., van den Bosch, F. C., & White, S. 2010, Galaxy Formation and Evolution
- Molero, M., Romano, D., Reichert, M., et al. 2021, MNRAS, 505, 2913, doi: [10.1093/mnras/stab1429](https://doi.org/10.1093/mnras/stab1429)
- Mösta, P., Roberts, L. F., Halevi, G., et al. 2018, ApJ, 864, 171, doi: [10.3847/1538-4357/aad6ec](https://doi.org/10.3847/1538-4357/aad6ec)
- Myeong, G. C., Vasiliev, E., Iorio, G., Evans, N. W., & Belokurov, V. 2019, MNRAS, 488, 1235, doi: [10.1093/mnras/stz1770](https://doi.org/10.1093/mnras/stz1770)
- Naidu, R. P., Conroy, C., Bonaca, A., et al. 2020, ApJ, 901, 48, doi: [10.3847/1538-4357/abae64](https://doi.org/10.3847/1538-4357/abae64)
- . 2021, arXiv e-prints, arXiv:2103.03251, <https://arxiv.org/abs/2103.03251>
- Neijssel, C. J., Vigna-Gómez, A., Stevenson, S., et al. 2019, MNRAS, 490, 3740, doi: [10.1093/mnras/stz2840](https://doi.org/10.1093/mnras/stz2840)
- Nishimura, N., Sawai, H., Takiwaki, T., Yamada, S., & Thielemann, F. K. 2017, ApJL, 836, L21, doi: [10.3847/2041-8213/aa5dee](https://doi.org/10.3847/2041-8213/aa5dee)
- Oliphant, T. 2006–, NumPy: A guide to NumPy, USA: Trelgol Publishing. <http://www.numpy.org/>

- Park, M. J., Yi, S. K., Peirani, S., et al. 2020, arXiv e-prints, arXiv:2009.12373.
<https://arxiv.org/abs/2009.12373>
- Paterson, K., Fong, W., Nugent, A., et al. 2020, ApJL, 898, L32, doi: [10.3847/2041-8213/aba4b0](https://doi.org/10.3847/2041-8213/aba4b0)
- Pérez, F., & Granger, B. E. 2007, Computing in Science and Engineering, 9, 21, doi: [10.1109/MCSE.2007.53](https://doi.org/10.1109/MCSE.2007.53)
- Perley, D. A., Fremling, C., Sollerman, J., et al. 2020, ApJ, 904, 35, doi: [10.3847/1538-4357/abbd98](https://doi.org/10.3847/1538-4357/abbd98)
- Pfeffer, J., Lardo, C., Bastian, N., Saracino, S., & Kamann, S. 2021, MNRAS, 500, 2514, doi: [10.1093/mnras/staa3407](https://doi.org/10.1093/mnras/staa3407)
- Pfeffer, J. L., Trujillo-Gomez, S., Kruijssen, J. M. D., et al. 2020, arXiv e-prints, arXiv:2003.00076.
<https://arxiv.org/abs/2003.00076>
- Placco, V. M., Sneden, C., Roederer, I. U., et al. 2021, linemake: Line list generator. <http://ascl.net/2104.027>
- Planck Collaboration, Aghanim, N., Akrami, Y., et al. 2018, arXiv e-prints, arXiv:1807.06209.
<https://arxiv.org/abs/1807.06209>
- Price-Whelan, A., Sipocz, B., Major, S., & Oh, S. 2017, adrn/gala: v0.2.1, doi: [10.5281/zenodo.833339](https://doi.org/10.5281/zenodo.833339)
- Price-Whelan, A. M. 2017, The Journal of Open Source Software, 2, doi: [10.21105/joss.00388](https://doi.org/10.21105/joss.00388)
- Reichert, M., Hansen, C. J., Hanke, M., et al. 2020, A&A, 641, A127, doi: [10.1051/0004-6361/201936930](https://doi.org/10.1051/0004-6361/201936930)
- Roederer, I. U., Sakari, C. M., Placco, V. M., et al. 2018, ApJ, 865, 129, doi: [10.3847/1538-4357/aadd92](https://doi.org/10.3847/1538-4357/aadd92)
- Romero-Shaw, I. M., Farrow, N., Stevenson, S., Thrane, E., & Zhu, X.-J. 2020, MNRAS, 496, L64, doi: [10.1093/mnras/slaa084](https://doi.org/10.1093/mnras/slaa084)
- Safarzadeh, M., Ramirez-Ruiz, E., Andrews, J. J., et al. 2019, ApJ, 872, 105, doi: [10.3847/1538-4357/aafe0e](https://doi.org/10.3847/1538-4357/aafe0e)
- Santoliquido, F., Mapelli, M., Giacobbo, N., Bouffanais, Y., & Artale, M. C. 2021, MNRAS, 502, 4877, doi: [10.1093/mnras/stab280](https://doi.org/10.1093/mnras/stab280)
- Schönrich, R. A., & Weinberg, D. H. 2019, MNRAS, 487, 580, doi: [10.1093/mnras/stz1126](https://doi.org/10.1093/mnras/stz1126)
- Siegel, D. M., Barnes, J., & Metzger, B. D. 2019, Nature, 569, 241, doi: [10.1038/s41586-019-1136-0](https://doi.org/10.1038/s41586-019-1136-0)
- Simonetti, P., Matteucci, F., Greggio, L., & Cescutti, G. 2019, MNRAS, 486, 2896, doi: [10.1093/mnras/stz991](https://doi.org/10.1093/mnras/stz991)
- Skúladóttir, Á., Hansen, C. J., Salvadori, S., & Choplin, A. 2019, A&A, 631, A171, doi: [10.1051/0004-6361/201936125](https://doi.org/10.1051/0004-6361/201936125)
- Skúladóttir, Á., & Salvadori, S. 2020, A&A, 634, L2, doi: [10.1051/0004-6361/201937293](https://doi.org/10.1051/0004-6361/201937293)
- Sneden, C., Cowan, J. J., & Gallino, R. 2008, ARA&A, 46, 241, doi: [10.1146/annurev.astro.46.060407.145207](https://doi.org/10.1146/annurev.astro.46.060407.145207)
- Sneden, C. A. 1973, PhD thesis, The University of Texas at Austin.
- Sobeck, J. S., Kraft, R. P., Sneden, C., et al. 2011, AJ, 141, 175, doi: [10.1088/0004-6256/141/6/175](https://doi.org/10.1088/0004-6256/141/6/175)
- Steinmetz, M., Matijević, G., Enke, H., et al. 2020, AJ, 160, 82, doi: [10.3847/1538-3881/ab9ab9](https://doi.org/10.3847/1538-3881/ab9ab9)
- The LIGO Scientific Collaboration, the Virgo Collaboration, Abbott, R., et al. 2021, arXiv e-prints, arXiv:2108.01045. <https://arxiv.org/abs/2108.01045>
- Ting, Y.-S., Freeman, K. C., Kobayashi, C., De Silva, G. M., & Bland-Hawthorn, J. 2012, MNRAS, 421, 1231, doi: [10.1111/j.1365-2966.2011.20387.x](https://doi.org/10.1111/j.1365-2966.2011.20387.x)
- Tsujimoto, T. 2021, ApJL, 920, L32, doi: [10.3847/2041-8213/ac2c75](https://doi.org/10.3847/2041-8213/ac2c75)
- van de Voort, F., Pakmor, R., Bieri, R., & Grand, R. J. J. 2021, arXiv e-prints, arXiv:2110.11963.
<https://arxiv.org/abs/2110.11963>
- Van der Swaelmen, M., Hill, V., Primas, F., & Cole, A. A. 2013, A&A, 560, A44, doi: [10.1051/0004-6361/201321109](https://doi.org/10.1051/0004-6361/201321109)
- VandenBerg, D. A., Brogaard, K., Leaman, R., & Casagrande, L. 2013, ApJ, 775, 134, doi: [10.1088/0004-637X/775/2/134](https://doi.org/10.1088/0004-637X/775/2/134)
- Vasiliev, E., & Baumgardt, H. 2021, MNRAS, 505, 5978, doi: [10.1093/mnras/stab1475](https://doi.org/10.1093/mnras/stab1475)
- Vasiliev, E., Belokurov, V., & Evans, W. 2021, arXiv e-prints, arXiv:2108.00010.
<https://arxiv.org/abs/2108.00010>
- Virtanen, P., Gommers, R., Oliphant, T. E., et al. 2020, Nature Methods, 17, 261, doi: <https://doi.org/10.1038/s41592-019-0686-2>
- Wehmeyer, B., Pignatari, M., & Thielemann, F. K. 2015, MNRAS, 452, 1970, doi: [10.1093/mnras/stv1352](https://doi.org/10.1093/mnras/stv1352)
- Weisz, D. R., Dolphin, A. E., Skillman, E. D., et al. 2014, ApJ, 789, 147, doi: [10.1088/0004-637X/789/2/147](https://doi.org/10.1088/0004-637X/789/2/147)
- Yong, D., Kobayashi, C., Da Costa, G. S., et al. 2021, Nature, 595, 223, doi: [10.1038/s41586-021-03611-2](https://doi.org/10.1038/s41586-021-03611-2)
- Yuan, Z., Myeong, G. C., Beers, T. C., et al. 2020, ApJ, 891, 39, doi: [10.3847/1538-4357/ab6ef7](https://doi.org/10.3847/1538-4357/ab6ef7)